ESTIMATION OF SPECIAL OPTICAL PROPERTIES OF A TRIANGULAR RING CAVITY

F. J. RAAB, S. E. WHITCOMB, 6 FEBRUARY 1992

Abstract

The optical-feedback and polarization-filtering properties of a three-mirror triangular ring cavity, and the irreducible fringe-visibility defect encountered in mode matching light between a triangular ring cavity and a linear cavity are evaluated. Numerical results are obtained for the prototype suspended-mirror mode cleaner currently under development.

I. INTRODUCTION

A three-mirror triangular ring cavity can be used to filter laser light in a similar manner to the commonly used two-mirror linear cavity. It has the advantage that it is an intrinsically low optical-feedback element which will purify the linear polarization state of the input light. These advantages are purchased at the cost of additional complexity and losses due to the extra mirror as well as some additional irreducible losses incurred in coupling light between the elliptical Gaussian mode of a triangular cavity and the normal circular Gaussian modes of linear cavities such as lasers and interferometers. The optical feedback from a triangular ring cavity is evaluated in Section II. The polarization filtering action of a triangular mode cleaner is evaluated in Section III. Section IV evaluates the irreducible fringe visibility defect for mode matching light between triangular and linear cavities. In each section, the results are numerically evaluated for the specific case of the prototype suspended-mirror mode cleaner (SMMC) currently under development for the initial LIGO interferometer.

II. OPTICAL FEEDBACK FROM A TRIANGULAR RING CAVITY

The optical feedback from a linear cavity is dominated by direct reflection from the input mirror and is typically between 0.1 and 1. For a ring cavity the light does not strike any of the mirrors at normal incidence and thus the optical feedback results from backscattering, (i.e., the scattering of light from the input mode into a mode that is spatially identical to the input mode but propagates in the opposite direction). Because the distribution function for this type of scattering (BRDF[1]) is strongly peaked at low angles of incidence, θ, a closed-area ring cavity design such as the proposed SMMC (which uses two flat mirrors at 45° incidence and one curved mirror at near-normal incidence) backscatters principally from a single mirror (Figure 1).

[1] J. C. Stover, Optical Scattering, McGraw-Hill, N.Y. (1990), pp 16–17, 86–87.

LIGO - T920004-00-R

The backscattered amplitude from the cavity can be obtained from the cavity-field rate equations:

$$\frac{2l}{c}\dot{E}_c = -(1-r^2)E_c + tE_i \tag{1}$$

$$\frac{2l}{c}\dot{E}_{cc} = -(1-r^2)E_{cc} + \sigma E_c \tag{2}$$

Here E_c is the circulating field, sourced by the transmitted input field, tE_i. E_{cc} is the counter-circulating field, sourced by the backscattered field from the curved mirror, σE_c. The field reflectivity of the flat mirrors used to couple light into and out from the cavity is r; we approximate the field reflectivity of the curved mirror as unity. The steady-state solutions (obtained by setting the left hand sides of equations (1) and (2) to zero) are:

$$E_c = \frac{tE_i}{1-r^2} \tag{3}$$

$$E_{cc} = \frac{\sigma E_c}{1-r^2} \tag{4}$$

The backscattered amplitude from the cavity is $E_{BS} = tE_{cc}$. Using $t^2 \simeq 1-r^2$ (assuming scattering and absorption are small compared to transmission) and $R = r^2$, we obtain for the backscattered power:

$$P_{BS} \simeq \frac{\sigma^2}{(1-R)^2}P_i \tag{5}$$

The power coupling between the circulating and counter-circulating beams due to scattering, is given by

$$\sigma^2 = G(\theta_o)\Omega_M, \tag{6}$$

where $G(\theta_o)$ is the BRDF evaluated at the angle θ_o between the reflected input and scattered output modes (i.e. twice the angle of incidence) and the solid angle of the input mode is given by

$$\Omega_M = \left(\frac{\lambda}{2\pi w_o}\right)^2 \tag{7}$$

The power backscattered from the cavity is then given by

$$P_{BS} = \frac{G(\theta_o)\Omega_M}{(1-R)^2}P_i \tag{8}$$

A reasonable model for the BRDF,[2] sketched in Figure 2, is

$$G(\theta) = \begin{cases} \dfrac{\alpha}{{\theta_1}^2}, & 0 \le \theta < \theta_1 \simeq 10^{-4} \text{ ; (I)} \\ \dfrac{\alpha}{\theta^2}, & \theta_1 \le \theta \le \theta_2 \simeq 10^{-1}\text{; (II)} \\ \dfrac{\alpha}{{\theta_2}^2}, & \theta_2 < \theta \le \dfrac{\pi}{2} \quad \text{; (III)} \end{cases} \tag{9}$$

The constant α is chosen such that

$$S = 2\pi \int_{o}^{\pi/2} G(\theta) \sin\theta d\theta \tag{10}$$

where S is the total integrated scattering. Since θ_1 and θ_2 are small, we can set $\sin\theta \simeq \theta$ in regions I and II. Performing the appropriate integrals and summing over all three regions we obtain:

$$S = 2\pi\alpha \left[\frac{1}{{\theta_2}^2} + ln\left(\frac{\theta_2}{\theta_1}\right)\right] \tag{11}$$

Taking the values $\theta_1 \simeq 10^{-4}, \theta_2 \simeq 10^{-1}$, we get[3] $S = 671\,\alpha$ or

$$\alpha \simeq 1.5 \times 10^{-3} S \tag{12}$$

For a typical value of $S = 100\text{ppm}$ (allowing for contamination of the mirror) we obtain a value of $\alpha \simeq 1.5 \times 10^{-7}$.

For a small area configuration $L_F \ll L_C$, we have $\theta_o \simeq L_F/L_C = 10^{-2}$, $G(\theta_o) = \alpha\left(\frac{L_C}{L_F}\right)^2$ so that

$$P_{BS} = \frac{\alpha}{(1-R)^2} \cdot \left(\frac{L_C}{L_F}\right)^2 \cdot \left(\frac{\lambda}{2\pi w_o}\right)^2 \cdot P_i \tag{13}$$

Substituting the appropriate values for the proposed mode cleaner ($L_F = 0.14m$, $L_C = 12.02m$, curved mirror radius $R_C = 17m, (1-R) = 2000ppm$), we obtain $w_o = 1.1 \times 10^{-3}m$ and $(P_{BS}/P_i) = 1.5 \times 10^{-6}$. The optical feedback from the triangular cavity, in this case -58 dB, can be compared to a typical value of -17 dB for a linear cavity with an input

2 R. Weiss, private communication.

3 It is interesting to note that the logarithmic term in equation (6) is merely a 7% correction to the overall scattering for these values of θ_1 and θ_2, and is small even for LIGO sized cavities. S is dominated by large angle scattering.

circulator, with an additional -35 dB provided by each Faraday isolator. For comparison the optical isolation between the mode cleaner and the main cavities in the current 40–m prototype (two circulators, one Faraday isolator, optical losses) is estimated to be -95 dB.

III. POLARIZATION FILTERING BY A TRIANGULAR RING CAVITY

In a linear two-mirror cavity with dielectric mirrors, the field is phase shifted by π upon each reflection, independent of its polarization. The net phase shift due to the mirror reflections alone (to be distinguished from the phase accumulated in propagation between mirrors) is zero (modulo 2π) after each round trip. This degeneracy with respect to polarization may be broken in a ring cavity where the mirrors are not used at normal incidence.[4] For planar ring cavities the net phase shifts introduced by the mirror reflections in a round trip through the cavity are $\phi_s = n\pi$ for S-polarization (normal to cavity plane), where n is the number of mirrors in the cavity, and $\phi_p = 0$, independent of the number of mirrors in the cavity. The resonance conditions for a triangular ring cavity are then:

$$2\pi n_s = \frac{4\pi L}{c}\nu_s + \psi^{(s)}_{lm} + \pi \tag{14}$$

$$2\pi n_p = \frac{4\pi L}{c}\nu_p + \psi^{(p)}_{lm} \tag{15}$$

where n_s and n_p are integers and ν_s and ν_p are the resonant frequencies for s and p polarized modes. Neglecting the possibility of polarization-dependent Guoy phase shifts (i.e. assuming $\psi^{(s)}_{lm} - \psi^{(p)}_{lm} = \psi$) we can approximate the mode frequencies as:

$$\nu_s = \frac{c}{2l} \cdot (n_s - 1/2 - \zeta) \tag{16}$$

$$\nu_p = \frac{c}{2l} \cdot (n_p - \zeta) \tag{17}$$

where $\zeta = \psi/2$. We see that at any of the cavity resonances only one polarization is resonant. A useful figure of merit is extinction ratio, defined as the cavity transmission for the favored polarization divided by the transmission for the disfavored polarization for a given mode. For the case of equal transmissions for the input and output mirrors (assuming full reflectivity for the third mirror) we obtain:

$$R_E = \left(\frac{1+R}{1-R}\right)^2 \tag{18}$$

where R is the reflectivity of the input (or output) mirror. For typical mode-cleaner mirrors (transmission T=2000 ppm, loss L=100 ppm) we obtain $R_E = 8 \times 10^5$. The polarization

[4] See, for instance, Jenkins and White, Fundamentals of Optics, McGraw-Hill. N.Y. (1957), pp 513–515.

filtering improves as the square of the finesse of the mode cleaner, but is independent of the mode cleaner length.[5]

IV. ASTIGMATISM AND FRINGE VISIBILITY

By inspection of Figure 1 we see that reflection symmetry requires that the beam waist occur midway between the two flat mirrors. The focussing properties of the curved mirror are, however, different for rays in the tangential and sagittal planes (plane of Figure 1 and plane perpendicular to Figure 1, respectively). This astigmatism results in a splitting of the mirror imaging equation into two forms:[6]

$$\frac{1}{S} + \frac{1}{S'_T} = -\frac{2}{R_C \cos\theta_i} = -\frac{2}{R_T} \tag{19}$$

$$\frac{1}{S} + \frac{1}{S'_S} = -\frac{2\cos\theta_i}{R_C} = -\frac{2}{R_S} \tag{20}$$

where S is the object distance, S'_S and S'_T are the imaging distances for tangential and sagittal rays, respectively, R_C is the actual curvature for the spherical mirror, θ_i is the angle of incidence (for the chief ray), and R_T, R_S are the effective mirror radii for tangential and sagittal ray focussing, respectively. The azimuthal symmetry breaking introduced by a nonzero θ_i results in an elliptical Gaussian beam waist with principal axes along the tangential and sagittal planes. For a cavity with $L_C \gg L_F$, this astigmatism is small and the two waist sizes are given by (see Appendix A):

$$w_{oT} = w_o\left[1 - \frac{\delta R}{4(R_C - L)} - \frac{3(\delta R)^2}{32(R_C - L)^2}\right] \tag{21}$$

$$w_{oS} = w_o\left[1 + \frac{\delta R}{4(R_C - L)} - \frac{3(\delta R)^2}{32(R_C - L)^2}\right] \tag{22}$$

Where L is the distance from the curved mirror to the beam waist, w_o is the circular waist size for the flat and curved mirrors in a linear resonator of length L, and δR is the change in effective mirror radius due to astigmatism. Subtracting equation (19) from (20), and assuming $\theta_i \ll 1$, we have

$$\delta R = \frac{R_S - R_T}{2} = \frac{R_C\theta_i^2}{2} \tag{23}$$

---

[5] Filtering of spatial variations on the light have a similar dependence on cavity length and finesse. This is not surprising since spatial variations and polarization impurities can only be transmitted on non-resonant modes.

[6] Jenkins and White, pg 95; Monk, Light, Principles and Experiments, 1st ed., McGraw-Hill, N.Y. (1937), pp 52 and 424.

The irreducible loss in visibility which occurs when mode matching this astigmatic elliptical beam into a linear Fabry-Perot cavity using spherical lenses is

$$\delta V_M = 1 - M_o \tag{24}$$

where M_o is the mode matching coefficient given by

$$M_o = \left| \int dxdy u_e(x,y) u_{oo}(x,y) \right|^2 \tag{25}$$

Here u_e is the transverse spatial dependence of the elliptical input mode waist and u_{oo} is the corresponding dependence of the circular waist of the linear resonator. In general we obtain

$$M_o = \frac{4{w_o}^2 w_{oS} w_{oT}}{({w_{oS}}^2 + {w_o}^2)({w_{oT}}^2 + {w_o}^2)} \tag{26}$$

where w_o is the circular beam waist and w_{oS} and w_{oT} are the major and minor axes of the elliptical Gaussian beam. This reduces to

$$M_o = \frac{4 w_{oS} w_{oT}}{(w_{oS} + w_{oT})^2} \tag{27}$$

for the case of optimized mode matching using spherical lenses $\left({w_o}^2 = w_{oS} w_{oT}\right)$. Substituting from equations (21) and (22), this becomes

$$M_o = 1 - \left[\frac{\delta R}{4(R_C - L)}\right]^2 \tag{28}$$

Using equations (23) and (24) we finally have

$$\delta V_M = \frac{1}{64} \frac{{\theta_i}^4}{(1 - L/R_C)^2} \tag{29}$$

For the resonator of Figure 1 with $L = 12.16m$, $\theta_i = 6 \times 10^{-3}$, we have $\delta V_M \simeq 6 \times 10^{-11}$ which is completely negligible.

APPENDIX A

DERIVATION OF ELLIPTICAL GAUSSIAN WAIST SIZE

We may calculate the beam shape by separately applying results for an azimuthally symmetric resonator separately to the tangential and sagittal planes.[7] For a symmetric linear resonator using spherical mirrors we have[8]

$$w_o = \left(\frac{L_e \lambda}{2\pi}\right)^{1/2} \tag{A.1}$$

$$L_e = [(2R_C - L)L]^{1/2} \tag{A.2}$$

where w_o is the circular beam waist radius, L_e is the length of the equivalent confocal resonator, λ is the wavelength of the light, and L is the separation between the two spherical mirrors of radius R_c. For a hemispherical linear resonator (a curved mirror and a flat) we replace L by $2L$ in equation (A.2) obtaining

$$L_e = 2[(R_C - L)L]^{1/2} \tag{A.3}$$

where L is now the separation between the curved mirror and the flat mirror (where the beam waist occurs). To generalize to the triangular ring cavity we use equation (A.3) where L is now the distance (along the light path) from the curved mirror to the midpoint between the flat mirrors. We separately calculate semi-major and semi-minor lengths of the elliptical Gaussian beam by substituting either R_S or R_T for R_C in equation (A.3) and then using equation (A.1).

For θ_i small, we have

$$R_T = R_C\left(1 - \frac{\theta_i^2}{2}\right) \tag{A.4}$$

$$R_S = R_C\left(1 + \frac{\theta_i^2}{2}\right) \tag{A.5}$$

We see that weaker focussing occurs in the sagittal plane so the major axis of the elliptical Gaussian beam occurs in this plane. We redefine

$$R_T = R_C - \delta R \tag{A.6}$$

7 A. Yariv, Quantum Electronics, 2nd ed, Wiley, N.Y. (1975), pp 123–127.

8 O. Svelto, Principles of Lasers, Plenum, N.Y. (1982), pp 128–132.

$$R_S = R_C + \delta R \tag{A.7}$$

where $\delta R = \frac{1}{2}(R_S - R_T) = \frac{R_C\theta^2}{2}$. We then obtain for the principal axes of the elliptical Gaussian:

$$w_{oT} = w_o\left[1 - \frac{\delta R}{4(R_C - L)} - \frac{3(\delta R)^2}{32(R_C - L)^2}\right] \tag{A.8}$$

$$w_{oS} = w_o\left[1 + \frac{\delta R}{4(R_C - L)} - \frac{3(\delta R)^2}{32(R_C - L)^2}\right] \tag{A.9}$$

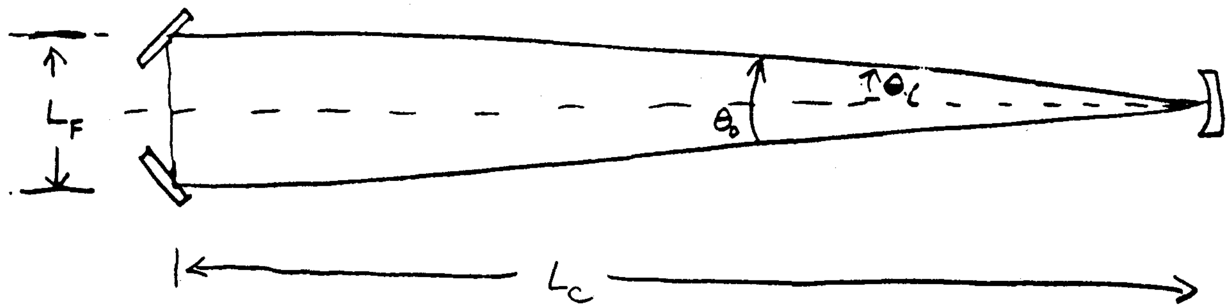

Figure 1. Triangular Ring Cavity Plan View.

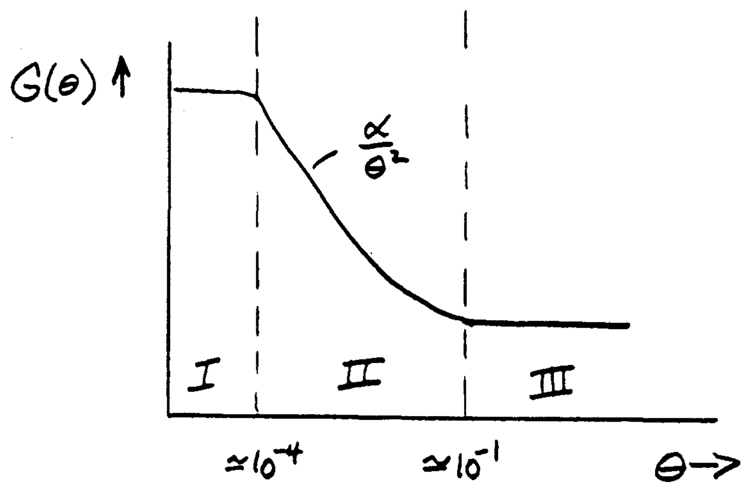

Figure 2. Model BRDF.